Supporting Information

Selective inhibition of *Rhizopus* eumelanin biosynthesis by novel natural product scaffold-based designs caused significant inhibition of fungal pathogenesis

Sameh S. M. Soliman[1,2,3 #, *], Rania Hamdy[1,3#], Samia A. Elseginy[4,5], Teclegiorgis Gebremariam[6], Alshaimaa M. Hamoda[1,7], Mohamed Madkour[1,8], Thenmozhi Venkatachalam[1], Mai N. Ershaid[1], Mohammad G Mohammad[1,8], Georgios Chamilos[9,10] and Ashraf S. Ibrahim[6,11,*]

Table of Contents

S1

Detailed synthesis of UOSC1-14

Synthesis of (cuminic acid) isopropyl benzoic acid 2. Cuminic acid was prepared from oxidation of cuminaldehyde in water with iodine as catalyst (10 mmol), NaOH (20 mmol) TBHP following a reported procedure [21]. ^{1}H-NMR (DMSO-d_6.δ):.δ): 1.21 (d, 6H, 2 CH_3 of isoproyl), 2.90 (q, 1H, CH of isopropyl), 7.34 (d , 2H, j= 8, ArH), 7.54 (d, 2H, j= 7.5, ArH).

General procedure for the synthesis ethyl 4-substituted benzoate (4, 5). A mixture of the appropriate 4-substituted benzoic acid **2, 3** (10 mmol), absolute ethanol (20 mL) and concentrated sulphuric acid (2 mL) was refluxed for 3 hours. Excess ethanol was distilled under reduced pressure and the resulting oil was rendered alkaline with aqueous sodium bicarbonate and extracted with methylene chloride (2× 50 mL). The combined organic extract was dried over anhydrous sodium sulphate and distilled under reduced pressure to give the corresponding ester in a yield of 68%.

General procedure for the synthesis of 4-substituted benzoic acid hydrazide (6, 7). To a solution of ethyl 4-substituted benzoate 4, 5 (10 mmol) in ethanol (10 mL), excess hydrazine monohydrate (5 mL) was added. The reaction mixture was refluxed for 24 hours, and left to cool to room temperature. The formed precipitate was collected by filtration, washed with water followed by cold ethanol to remove excess hydrazine and left to dry to give the corresponding acid hydrazide.

4-Isopropyl-benzoic acid hydrazide **6,** Yeild 85%, ^{1}H-NMR (DMSO-d_6.δ): 1.21 (d, 6H, 2 CH_3 of isoproyl), 2.93 (m, 1H, CH of isopropyl), 4.45 (s, 2H, NH_2), 7.31 (d, 2H, j= 8, ArH), 7.54 (d, 2H, j= 6.5, ArH), 9.67 (s, 1H, NH).

4-tert-Butyl-benzoic acid hydrazide **7,** Yeild 87% , ^{1}H-NMR (DMSO-d_6.δ): 1.29 (s, 9H, tert-butyl), 4.45 (s, 2H, NH_2), 7.45 (d , 2H, j= 8.5, ArH), 7.75 (d, 2H, j= 6.5, ArH), 9.68 (s, 1H, NH).

General procedure for the synthesis of 3-Substituted-4-(4 substituted-benzyloxy) benzaldehyde R (1-9). To a mixture of substituted benzyl chloride **8-10** (10 mmol), K_2CO_3(12 mmol) and KI (trace amount) in 20 mL acetonitrile, 3-substituted-4-hydroxybenzaldehde **11-13** was added drop wise under inert nitrogen and stirred overnight, evaporate under reduced pressure. The crude mixture was quenched with water and the

resulting un-dissolved solid was collected by filtration, washed with water, dried and re-crystallized from aqueous ethanol to give the titled compound**.**

3-Methoxy-4-(4-methyl-benzyloxy)-benzaldehyde **R1,** Yield 75%, ^{1}H-NMR (DMSO-d_6 .δ): 2.31 (s, 3H, CH_3), 3.83 (s, 3H, OCH_3), 5.17 (s, 2H, CH_2), 7.21 (d, 2H, j= 8, ArH), 7.27 (d, 1H, j= 8, ArH), 7.34 (d, 2H, j= 8, ArH), 7.41 (d, 1H, j= 2, ArH), 7.55 (dd , 1H, j= 8, ArH), 9.84 (s, 1H, CHO).

3-Bromo-4-(4-methyl-benzyloxy)-benzaldehyde **R2,** Yield 79%, ^{1}H-NMR (DMSO-d_6 .δ) : 2.32 (s, 3H, CH_3), 5.30 (s, 2H, CH_2), 7.22 (d, 2H, j= 8, ArH), 7.39 (m, 3H, ArH), 7.93 (d , 1H, j= 8.5, ArH), 8.12 (d, 1H, j= 2, ArH), 9.85 (s, 1H, CHO).

3-Chloro-4-(4-methyl-benzyloxy)-benzaldehyde **R3**, Yield 67%, ^{1}H-NMR (DMSO-d6. δ): 2.31 (s, 3H, CH_3), 5.30 (s, 2H, CH_2), 7.22 (d, 2H, j= 8, ArH), 7.36 (d, 2H, j= 8, ArH), 7.44 (d, 1H, j= 8.5, ArH), 7.87 (dd, 1H, j=8.5, ArH), 7.96 (d, 1H, j= 2, ArH), 9.86 (s, 1H, CHO).

3-Chloro-4-(4-trifluoromethyl-benzyloxy)-benzaldehyde **R4**, Yield 69%, ^{1}H-NMR (DMSO-d6 . δ) : 5.48 (s, 2H, CH_2), 7.45 (d, 1H, j= 8.5, ArH), 7.71 (d, 2H, j= 8, ArH), 7.81 (d, 2H, j= 8.5, ArH), 7.91 (dd, 1H, j= 8.5, ArH), 8.01 (d, 1H, j= 2, ArH), 9.88 (s, 1H, CHO).

3-Methoxy-4-(4-trifluoromethyl-benzyloxy)-benzaldehyde **R5**, Yield 69%, ^{1}H-NMR (DMSO-d6 . δ) : 3.86 (s, 3H, OCH_3), 5.35 (s, 2H, CH_2), 7.25 (d, 1H, j= 8, ArH), 7.44 (d , 1H, j= 2, ArH), 7.56 (dd, 1H, j= 8.5, ArH), 7.68 (d, 2H, j= 8.5, ArH), 7.79 (d, 2H, j= 8, ArH), 9.85 (s, 1H, CHO).

3-Bromo -4-(4-trifluoromethyl-benzyloxy)-benzaldehyde **R6**, Yield 72%, ^{1}H-NMR (DMSO-d6 . δ): 5.48 (s, 2H, CH_2), 7.41 (d , 1H, j= 8, ArH), 7.72 (d, 2H, j= 8.5, ArH), 7.81 (d, 2H, j= 8, ArH), 7.95 (dd, 1H, j= 8.5, ArH), 8.15 (d, 1H, j= 2, ArH), 9.87 (s, 1H, CHO).

3-Bromo-4-(3-trifluoromethyl-benzyloxy)-benzaldehyde **R7**, Yield 74%, ^{1}H-NMR (DMSO-d6 . δ) : 5.46 (s, 2H, CH_2), 7.42 (d, 1H, j= 8.5, ArH), 7.73 (m, 2H, ArH), 7.81 (d, 1H, j= 7.5, ArH), 7.89 (s, 1H, ArH), 7.95 (dd, 1H, j= 8.5, ArH), 8.15 (d, 1H, j= 2, ArH) 9.84 (s, 1H, CHO).

3-Methoxy-4-(3-trifluoromethyl-benzyloxy)-benzaldehyde **R8,** Yield 79%, ^{1}H-NMR (DMSO-d6 . δ): 3.86 (s, 3H, OCH_3), 5.34 (s, 2H, CH_2), 7.28 (d, 1H, j= 8.5, ArH), 7.44 (d, 1H, j= 2, ArH), 7.57 (dd, 1H, j= 8.5, ArH), 7.67 (m, 1H, ArH), 7.73 (d, 1H, j= 7.5, ArH), 7.75 (d, 1H, j= 7.5, ArH), 7.85 (s, 1H, ArH). 9.86 (s, 1H, CHO).

3-Chloro-4-(3-trifluoromethyl-benzyloxy)-benzaldehyde **R9,** Yield 69%, ^{1}H-NMR (DMSO-d6. δ): 5.46 (s, 2H, CH_2), 7.49 (d, 1H, j= 8.5, ArH), 7.70 (m, 1H, ArH), 7.76 (d, 1H, j= 8, ArH), 7.82 (d, 1H, j=7.5, ArH), 7.88 (s, 1H, ArH), 7.93 (dd, 1H, j= 8.5, ArH), 8.0 (d, 1H, j= 2, ArH), 9.88 (s, 1H, CHO).

General procedure for the synthesis 4-Substituted-benzoic acid [3-substituted-4-(4-substituted-benzyloxy)-benzylidene]-hydrazide UOSC (1-14). A mixture of the acid hydrazide (6-7) (10 mmol) and appropriate aromatic aldehydes (10 mmol), **R (1-9)**, in glacial acetic acid 6 mL was heated at reflux for 3-4 hrs till the reaction was completed. The reaction was monitored by TLC. The reaction mixture was concentrated under reduce pressure, cooled and the solid obtained was filtered and crystallized.

4-Isopropyl-benzoic acid [3-methoxy-4-(4-methyl-benzyloxy)-benzylidene]-hydrazide **UOSC-1**, Yield 75%, MP: 185-187. ^{1}H-NMR (DMSO-d_6. δ): 1.24 (d, 6H, 2 CH_3 of isopropyl), 2.50 (s, 3H, CH_3), 2.95 (m, 1H, CH of isopropyl), 3.83 (s, 3H, OCH_3), 5.09 (s, 2H, CH_2), 7.12 (d, 1H, j= 8.5, ArH), 7.21 (m, 3H, ArH), 7.37 (m, 5H, ArH), 7.85 (d, 2H, j= 8.5, ArH), 8.37 (s, 1H, CH), 11.66 (s, 1H, NH). ^{13}C NMR (DMSO-d6.δ): 20.79, 23.64, 39.04, 55.51, 69.78, 108.47, 113.06, 121.74, 126.39, 127.36, 127.72, 128.01, 129.0, 131.2, 133.75, 137.23, 147.72, 149.38, 149.75, 152.36, 162.95. MS analysis for $C_{26}H_{28}N_2O_3$, Calcd mass 416.21, found (m/z, ESI+) (M^+ +1): 416.99.

4-Isopropyl-benzoic acid [3-methoxy-4-(3-trifluoromethyl-benzyloxy)-benzylidene]-hydrazide **UOSC-2**, Yield 68%, MP: 145-147. ^{1}H-NMR (DMSO-d_6. δ): 1.23 (d, 6H, 2 CH_3 of isoproyl), 2.96 (m, 1H, CH of isopropyl), 3.85 (s, 3H, OCH_3), 5.33 (s, 2H, CH_2), 7.15 (d, 1H, j= 8, ArH), 7.21 (d, 1H, j= 7.5, ArH), 7.40 (d, 3H, j= 7.5, ArH), 7.66 (m, 1H, ArH), 7.72 (d, 1H, j= 7.5, ArH), 7.79 (d, 1H, j=7.5, ArH), 7.85 (d, 3H, j=8, ArH), 8.38 (s, 1H, CH), 11.68 (s, 1H, NH). ^{13}C NMR (DMSO-d6.δ): 23.63, 33.44, 55.57, 69.17, 108.63, 113.371, 121.66, 123.12, 124.64, 125.81, 127.73, 128.2, 129.68, 130.09, 131.81, 138.39, 147.61, 149.44, 152.38, 162.98, 191.42 MS analysis for $C_{26}H_{25}F_3N_2O_3$, Calcd mass 470.18, found (m/z, ESI+) (M^+ +1): 470.75

4-tert-Butyl-benzoic acid [3-chloro-4-(4-methyl-benzyloxy)-benzylidene]-hydrazide **UOSC-3**, Yield 89%, MP: 129-131. ^{1}H-NMR (DMSO-d_6 .δ): 1.32 (s, 9H, t-butyl), 2.32 (s, 3H, CH_3), 5.23 (s, 2H, CH_2), 7.23 (d, 2H, j= 8, ArH), 7.34 (d, 1H, j= 8.5, ArH), 7.38 (d, 2H, j= 8, ArH), 7.54 (d, 2H, j= 8.5, ArH), 7.64 (d, 1H, j= 7.5, ArH), 7.85 (m, 3H, ArH), 8.37 (s, 1H, CH), 11.78 (s, 1H, NH). ^{13}C NMR (DMSO-d6.δ): 20.795, 30.924, 70.165, 114.388, 122.183, 125.257, 127.493, 128.177, 129.093, 130.646, 133.239, 137.386,

145.889, 154.644, 154.877, 163.019, 206.516. MS analysis for $C_{26}H_{27}ClN_2O_2$, Calcd mass 434.18, found (m/z, ESI+) (M^+ +1):435.18.

4-tert-Butyl-benzoic acid [3-chloro-4-(3-trifluoromethyl-benzyloxy)-benzylidene]-hydrazide **UOSC-4**, Yeild 65%, MP: 178-180. ^{1}H-NMR (DMSO-d_6 .δ): 1.32 (s, 9H, t-butyl), 5.4 (s, 2H, CH_2), 7.35 (d, 1H, j= 8.5, ArH), 7.55 (d, 2H, j= 8.5, ArH), 7.68 (m, 3H, ArH), 7.80 (m, 5H, ArH), 8.37 (s, 1H, ArH), 11.80 (s, 1H, NH). ^{13}C NMR (DMSO-d6.δ): 30.935, 69.332, 114.44, 122.201, 123.100, 123.966, 124.783, 125.276, 127.509, 127.962, 128.547, 129.125, 129.628, 129.737, 130.632, 131.528, 137.898, 145.806, 154.578, 163.045. MS analysis for $C_{26}H_{24}ClF_3N_2O_2$, Calcd mass: 488.15

4-Isopropyl-benzoic acid [3-bromo-4-(4-methyl-benzyloxy)-benzylidene]-hydrazide **UOSC-5**, Yeild 65%, MP: 180-182. ^{1}H-NMR (DMSO-d_6 .δ): 1.23 (d, 6H, 2 CH_3 of isopropyl), 2.50 (s, 3H, CH_3), 2.98 (m, 1H, CH of isopropyl), 5.22 (s, 2H, CH_2), 7.23 (d, 2H, j= 8, ArH), 7.30 (d, 1H, j= 8.5, ArH), 7.39 (m, 4H, ArH), 7.68 (d, 1H, j= 7.5, ArH), 7.85 (d, 2H, j= 8, ArH), 7.98 (s, 1H, ArH), 8.35 (s, 1H, CH), 11.78 (s, 1H, NH). ^{13}C NMR (DMSO-d6.δ): 20.80, 23.65, 56.06, 70.22, 111.82, 114.20, 126.413, 127.63, 127.77, 128.19, 128.65, 129.09, 130.86, 131.01, 133.28, 137.34, 145.75, 152.48, 155.76, 163.05. MS analysis for $C_{25}H_{25}BrN_2O_2$, Calcd mass 464.11, found (m/z, ESI+) (M^+ +1): 465.38.

4-tert-Butyl-benzoic acid [3-methoxy-4-(4-methyl-benzyloxy)-benzylidene]-hydrazide **UOSC-6,** Yield 74%, MP: 174-176. ^{1}H-NMR (DMSO-d_6 .δ): 1.32 (s, 9H, t-butyl), 2.32 (s, 3H, CH_3), 3.84 (s, 3H, OCH_3), 5.09 (s, 2H, CH_2), 7.12 (d, 1H, j= 8.5, ArH), 7.21 (m, 3H, ArH), 7.35 (m, 3H, ArH), 7.53 (d, 2H, j= 8.5, ArH), 7.85 (d, 2H, j= 8.5, ArH), 8.37 (s, 1H, CH), 11.66 (s, 1H, NH). ^{13}C NMR (DMSO-d6.δ): MS analysis for $C_{27}H_{30}N_2O_3$, Calcd mass 430.23, found (m/z, ESI+) (M^+ +1): 431.99.

4-tert-Butyl-benzoic acid [3-bromo-4-(4-trifluoromethyl-benzyloxy)-benzylidene]-hydrazide **UOSC-7**, Yield 85%, ^{1}H-NMR (DMSO-d_6. δ): 1.32 (s, 9H, t-butyl), 5.40 (s, 2H, CH_2), 7.29 (d, 1H, j= 8.5, ArH), 7.54 (d, 2H, j= 8.5, ArH), 7.73 (m, 3H, ArH), 7.83 (m, 4H, ArH), 8.01 (s, 1H, ArH), 8.36 (s, 1H, CH), 11.81 (s, 1H, NH). ^{13}C NMR (DMSO-d6.δ): 30.96, 34.75, 69.4, 111.79, 114.22, 123.18, 125.32, 125.50, 127.54, 127.86, 128.29, 128.40, 128.65, 129.0, 130.62, 131.0, 141.27, 145.73, 154.75, 155.46, 163.1. MS analysis for $C_{26}H_{24}BrF_3N_2O_2$, Calcd mass 532.10 , found (m/z, ESI+) (M^+ +1): 533.12.

4-tert-Butyl-benzoic acid [3-methoxy-4-(3-trifluoromethyl-benzyloxy)-benzylidene]-hydrazide **UOSC-8**, Yield 79%, MP: 167-169. ^{1}H-NMR (DMSO-d_6 .δ): 1.32 (s, 9H, t-butyl), 3.85 (s, 3H, OCH_3), 5.26 (s, 2H,

CH_2), 7.15 (d, 1H, j= 8.5, ArH), 7.21 (d, 1H, j= 7.5, ArH), 7.39 (s, 1H, ArH), 7.55 (d, 2H, j= 8, ArH), 7.68 (m, 1H, ArH), 7.73 (d, 1H, j=7.5, ArH), 7.79 (d, 1H, j=7.5, ArH), 7.85 (m, 3H, ArH), 8.39 (s, 1H, CH), 11.69 (s, 1H, NH). ^{13}C NMR (DMSO-d6.δ): 30.97, 55.64, 69.18, 108.73, 113.42, 121.78, 124.22, 124.68, 124.74, 125.32, 127.53, 127.87, 129.15, 129.40, 130.80, 131.87, 138.44, 147.74, 149.47, 154.67, 163.14. MS analysis for $C_{27}H_{27}F_3N_2O_3$, $_{Calcd}$ mass 484.51, found (m/z, ESI+) (M^+ +1): 485.15.

4-tert-Butyl-benzoic acid [3-bromo-4-(4-methyl-benzyloxy)-benzylidene]-hydrazide **UOSC-9**, Yield 65%, MP: 188-190. ^{1}H-NMR (DMSO-d_6 .δ): 1.32 (s, 9H, t-butyl), 2.31 (s, 3H, CH_3), 5.16 (s, 2H, CH_2), 7.23 (d, 2H, j= 8, ArH), 7.30 (d, 1H, j= 9, ArH), 7.39 (d, 2H, j= 8, ArH), 7.53 (d, 2H, j= 8, ArH), 7.69 (d, 1H, j= 7.5, ArH), 7.85 (d, 2H, j= 8.5, ArH), 7.98 (s, 1H, ArH), 8.35 (s, 1H, CH), 11.79 (s, 1H, NH). ^{13}C NMR (DMSO-d6.δ): 20.81, 30.94, 34.73, 70.23, 111.82, 114.23, 125.28, 127.50, 127.65, 128.20, 129.06, 129.10, 130.64, 130.87, 133.29, 137.35, 145.77, 154.67, 155.75, 163.05. MS analysis for $C_{26}H_{27}BrN_2O_2$, Calcd mass 479.41, found (m/z, ESI+) (M^+ +1):480.81.

4-tert-Butyl-benzoic acid [3-methoxy-4-(4-trifluoromethyl-benzyloxy)-benzylidene]-hydrazide **UOSC-10**, Yield 79%, ^{1}H-NMR (DMSO-d_6 .δ): 1.32 (s, 9H, t-butyl), 3.86 (s, 3H, OCH_3), 5.27 (s, 2H, CH_2), 7.12 (d , 1H, j= 8, ArH), 7.78 (d, 1H, j= 8.5, ArH), 7.4 (s, 1H, ArH), 7.54 (d, 2H, j= 8.5, ArH), 7.69 (d, 2H, j=8, ArH), 7.78 (d, 2H, j=8.5, ArH), 7.85 (d, 2H, j=8.5, ArH), 8.39 (s, 1H, CH), 11.68 (s, 1H, NH). ^{13}C NMR (DMSO-d6.δ): 30.96, 39.00, 69.16, 108.72, 112.83, 121.8, 113.29, 121.80, 123.23, 125.40, 125.86, 127.54, 127.84, 128.14, 130.15, 141.79, 147.75, 149.44, 152.89, 154.68, 163.16. MS analysis for $C_{27}H_{27}F_3N_2O_3$, Calcd mass 484.20, found (m/z, ESI+) (M^+ +1):484.91.

4-Isopropyl-benzoic acid [3-chloro-4-(4-methylbenzyloxy)-benzylidene]-hydrazide **UOSC-11**, Yeild 70%, MP: 189-191. ^{1}H-NMR (DMSO-d_6 .δ): 1.23 (d, 6H, 2 CH_3 of isopropyl), 2.31 (s, 3H, CH_3), 2.95 (m, 1H, CH of isopropyl), 5.22 (s, 2H, CH_2), 7.23 (d, 2H, j= 8, ArH), 7.36 (m, 5H, ArH), 7.65 (d, 1H, j= 7.5, ArH), 7.83 (m, 3H, ArH), 8.36 (s, 1H, CH), 11.78 (s, 1H, NH). ^{13}C NMR (DMSO-d6.δ): 20.86, 23.70, 30.77, 33.50, 70.24, 114.46, 126.50, 127.59, 127.83, 127.93, 128.21, 129.18, 131.03, 133.29, 137.49, 146.02, 152.60, 154.95, 163.18. MS analysis for $C_{25}H_{25}ClN_2O_2$, Calcd mass 420.16, found (m/z, ESI+) (M^+ +1): 420.82.

4-tert-Butyl-benzoic acid [3-chloro-4-(4-trifluoromethyl-benzyloxy)-benzylidene]-hydrazide **UOSC-12**, Yield 69%, ^{1}H-NMR (DMSO-d_6 .δ): 1.32 (s, 9H, t-butyl), 5.47 (s, 2H, CH_2), 7.34 (d, 1H, j= 9, ArH), 7.55

(d, 2H, j= 8.5, ArH), 7.72 (m, 3H, ArH), 7.82 (d, 3H, j= 8.5, ArH), 7.85 (d, 2H, j= 7.5, ArH), 8.37 (s, 1H, CH), 11.80 (s, 1H, NH). ^{13}C NMR (DMSO-d6.δ): 31.00, 34.82, 69.43, 114.45, 122.37, 123.26, 125.41, 125.59, 127.63, 128.11, 128.59, 128.63, 128.84, 130.67, 141.30, 146.04, 154.71, 154.89, 163.35. MS analysis for $C_{26}H_{24}ClF_3N_2O_2$, Calcd mass 488.15, found (m/z, ESI+) (M^+ +1):489.23.

4-Isopropyl-benzoic acid [3-bromo-4-(3-trifluoromethyl-benzyloxy)-benzylidene]-hydrazide **UOSC-13**, Yield 68%, MP: 175-177. ^{1}H-NMR (DMSO-d_6 .δ): 1.23 (d, 6H, 2 CH_3 of isopropyl), 2.95 (m, 1H, CH of isopropyl), 5.39 (s, 2H, CH_2), 7.31 (d, 1H, j= 8.5, ArH), 7.39 (d, 2H, j= 8, ArH), 7.70 (m, 3H, ArH), 7.82 (m, 3H, ArH), 7.91 (s, 1H, ArH), 8.15 (s, 1H, ArH), 8.36 (s, 1H, CH), 11.80 (s, 1H, NH). ^{13}C NMR (DMSO-d6.δ): 23.64, 39.51, 69.68, 111.95, 114.224, 123.77, 125.28, 126.42, 127.80, 128.25, 129.75, 130.95, 130.99, 131.35, 134.07, 137.52, 145.70, 152.52, 155.46, 158.88, 163.12, 190.60. MS analysis for $C_{25}H_{22}BrF_3N_2O_2$, Calcd mass 518.08, found (m/z, ESI+) (M^+ +1): 520.86

4-tert-Butyl-benzoic acid [3-bromo-4-(3-trifluoromethyl-benzyloxy)-benzylidene]-hydrazide **UOSC-14**, Yield 75%, ^{1}H-NMR (DMSO-d_6 .δ): 1.32 (s, 9H, t-butyl), 5.39 (s, 2H, CH_2), 7.32 (d , 1H, j= 8.5, ArH), 7.55 (d, 2H, j= 8.5, ArH), 7.71 (m, 3H, ArH), 7.86 (m , 4H, ArH), 8.01 (s, 1H, ArH), 8.37 (s, 1H, CH), 11.81 (s, 1H, NH).^{13}C NMR (DMSO-d6. δ): 30.89, 34.67, 69.35, 111,76, 114.21, 123.06, 123.80, 124.67, 125.22, 128.17, 128.83, 129.02, 129.34, 129.65, 130.61, 130.92, 131.32, 137.91, 145.62, 154.62, 155.41, 163.00. MS analysis for $C_{26}H_{24}BrF_3N_2O_2$, Calcd mass 533.38, found (m/z, ESI+) (M^+ +1): 535.20.

S2

Detailed computational modelling studies of UOSC-1, 2, 13 and 14 compared to kojic acid

To confirm the selectivity of UOSC-1, 2, 13, and 14 to the fungal, but not the human tyrosinase, in depth docking studies for the interaction of UOSC-1, 2, 13, and 14 within the hydrophobic binding pocket of mushroom tyrosinase (PDB:2Y9X) was performed in comparison to their interaction within human tyrosinase (PDB:5M8M) [24]. These binding interactions were further compared to the interaction of the enzyme with its native ligands, tropolone and kojic acid. Furthermore, the binding mode and binding energies were investigated using Molecular Operating Environment (MOE)[25] and playmolecule [26] software, respectively.

Compared to the enzyme's bindings modes to troplone and kojic acid (**Supplementary Figure 1A**), the binding mode of UOSC-1 (observed IC_{50} = 4.287µg) showed that methyl phenyl group buried in the active site in the vicinity to copper ion which facilitate the interaction of O-atom of OCH_3 with NH-Val283 and forming a bond in a distance of 3.7Å. Moreover, methyl phenyl group showed π-π stacking with His 263 (ligand of Cu ion), and π–alkyl stacking with Ser282 and Gly281.Methoxy phenyl group showed parallel-displaced π-π stacking with Phe264. The carbonyl group of the compound illustrated electrostatic interactions with His85. The isopropyl phenyl group showed hydrophobic interactions with Glu322, Ala323 and Thr324 (**Supplementary Figure 1B**). However, snapshot of molecular dynamics of the compound showed 3H-bonds with the active site (**Supplementary Figure 1C**).

UOSC-2 (IC_{50}= 3.484), showed two H-bonds with the residues of the pocket site, the O-atom of C=O group formed an H-bond with the H-atom of His244 (reserved residue) at distance 3.1Å, and the O-atom of OCH_3 formed another H-bond with NH-Val248 at distance 3.8Å. The isopropyl phenyl moiety was deeply buried in the back hydrophobic pocket near the copper ions, surrounded by the hydrophobic residue Phe264, and hydrophobic part of Met280, Ser282 and Val283. The isopropyl phenyl moiety exhibited T-shaped edge-to-face π-π stacking with copper ion ligand residues His85, parallel-displaced π-π stacking between phenyl group and Phe264, and □□alkyl stacking between isopropyl group and Val283 (**Supplementary Figure 1D**). The methoxy phenyl group showed electrostatic

interactions with the negative amino acid of Glu322, while tri-flour phenyl group showed □□alkyl interactions with Ala264, Val247 and Val248 (**Supplementary Figure 1D**). The binding mode of UOSC-2 showed that phenylisopropyl group occupied the same position of kojic acid and /or tropolone, while the other part of the molecule extended in the entrance of the binding site, thus occupied the entire pocket in addition to multiple interactions (H-bond, electrostatic and □□□alkyl) with the pocket residues. These binding characteristics of the compound may explain its superiority as anti-melanin compared to kojic acid.

UOSC-13 (IC_{50} = 4.46), in which the methoxy group of UOSC-2 was replaced by Br resulted in different binding mode (**Supplementary Figure 1E**). The binding of UOSC-13 moved away from the copper ions active site, although $3CF_3$-phenyl still buried in the back binding pocket illustrating a π alkyl stacking interactions with Val238 and Asn260, and a face-to-edge π-π stacking with His244 (reserved residue). In contrast, 3-CF3 group showed electrostatic interactions with N-atom of His259 (Cu ion ligand) and NH of Val283 (key residue). The Br-phenyl group showed πalkyl stacking with Val248 and π-π edge-to-face stacking with Phe264 (key residue). The flexible carbonyl hydrazide formed 3H-bonds with the basic amino acid Arg268 at distances which stabilizes the molecule within the active site. The isopropyl phenyl showed hydrophobic interactions with hydrophobic residues Pro270, Asp273 and Leu275.

UOSC-14 (IC_{50}=5.300) showed a binding mode similar to UOSC-13, as the 3-CF_3-phenyl group moved a small distance away from the copper ions centre. The phenyl group of $3CF_3$-phenyl moiety was located between His259 and His263 (copper ligand ions) and showed π-π stacking with former residues and Phe264 (**Supplementary Figure 1F**). Furthermore, the CF_3-phenyl showed π alkyl interactions with Ser260, Ser282 and Val283 (key residues). The Cl-phenyl group showed π-π edge-to-face stacking with His244 (reserved residue) and π alkyl stacking with Val248 (**Supplementary Figure 1F**). Snapshot of MD simulation of UOSC-14 showed that it formed H-bonds with Asn260 and His244 at distance 3.2Å (**Supplementary Figure 1G**).

In summary, UOSC-1, 2, 13 and 14 showed promising anti-melanin activity due their excellent binding mode within the fungal (mushroom) tyrosinase active site. The 4 compounds buried beside copper ions active site, despite of UOSC-13 and 14 being displaced away by a small distance. The four compounds showed π-π stacking with copper

ions ligands (His61, His 85, His259, and His263) which may lead to a change in the geometry of copper ions centre and a disturbance in the redox reactions of tyrosinase. The four compounds illustrated strong interactions with the key and reserved residues of the hydrophobic pocket site including Hiss244, Val248 and Phe264. Moreover, the binding mode of UOSC-1 and 2 showed that both can occupy the active centre similar to the native ligand. Both compounds were very close to the copper ions, while the remaining of the compounds' structures was extended in the binding pocket, making these two compounds as the most promising fungal tyrosinase inhibitors (**Supplementary Figure 1H**).

Co-crystallization of kojic acid with human tyrosinase shows a close contact to Zn atom active site in a distance of 3.3Å-3.6Å, and a H-bond formed between O-atom of C=O group and the OH of the key residue Ser394 at distance 2.9Å. Kojic acid showed stacking interaction with His381 (key residue) (**Supplementary Figure 2A**). Compared to kojic acid, UOSC-1, 2, 13 and 14 moved far away from the Zn binuclear active site of the human tyrosinase (**Supplementary Figure 2A-E**).

To further predict the possible binding mode for each compound within the pocket site of mushroom tyrosinase, the binding free energy (ΔGBind) and the binding affinity pKd were determined [27, 28] (**Table 1**). It was found that the four compounds showed binding energies less than the reference compound kojic acid = -5.78 and higher binding affinity than kojic acid (pKd=4.28). UOSC-2 which showed the best IC_{50}=3.49 illustrated the lowest free binding energy (-9.13Kcal/mol) and the best binding affinity (pKd= 6.76). In comparison to mushroom tyrosinase, the binding energies and binding affinities of the four compounds within the human tyrosinase were very high and very low, respectively (**Table 1**). This result is in agreement with the concept that a compound with the best IC_{50} should exhibit the lowest binding energy [28]. The results confirmed that the newly-designed derivatives exhibited good binding mode which conformed to their lowest binding energies and high binding affinity than kojic acid. Furthermore, the orientation of the four compounds within human tyrosinase was far away of the active site and this is confirmed with the higher binding energies; explaining the selectively of the newly-designed UOSC-1, 2, 13 and 14 within mushroom tyrosinase.

Molecular dynamics **(**MD) simulations was carried out to further confirm the accuracy of docking results and to obtain more accurate ligand-protein model in a case close to the natural conditions and to explore the key residues at the active site of the enzyme [29]. Docking of UOSC-1, 2, 13 and 14 with the enzyme was tested using MD

simulation for 10ns. The MD simulations of the produced four complexes with the mushroom tyrosinase were checked for root mean square deviation (RMSD) to confirm the stability of the protein-inhibitors in the solvent system. The four complexes showed low RMSD values (0.15nm) (**Supplementary Figure 3A-C**). Furthermore, the complexes produced from UOSC-2, 13, and 14 showed smooth RMSD curves, which are less than or equal to RMSD of the enzyme alone, while RMSD of UOSC-1 jumped suddenly from 0.14 nm at 2ns to 0.17nm and stayed stable till the end of the dynamics study (**Supplementary Figure 3A**). UOSC-2, the most promising fungal tyrosinase inhibitor, reached the equilibrium at 1ns with ~0.14 nm RMSD which is less than the enzyme alone (**Supplementary Figure 3B**). These results indicate that the most stable form of mushroom tyrosinase occurs in the presence of aforementioned inhibitors in particular UOSC-2.

The Root mean square fluctuation (RMSF) plot of the Cα atom of each residue in the Hits-tyrosinase complexes was calculated to reveal the flexibility of mushroom tyrosinase backbone (**Supplementary Figure 3D-G**). The high RMSF value indicates more flexibility, whereas the low RMSF value shows limited movements during the simulation in relation to its average position over time [29]. The results showed that the RMSF of the Hits–tyrosinase complexes was high (~0.4 nm) with the first 100 residues, indicating the high flexibility of this part. The remaining residues showed low RMSF value ~0.2nm, particularly the binding pocket residues 200-300 (**Supplementary Figure 3E and G**). The low flexibility of the binding pocket residues indicates the stability of the enzyme due to the presence of the inhibitors. Furthermore, the RMSF of UOSC-1 and 2 with residues between 240-250 in the binding pocket is lower than the protein alone (**Supplementary Figure 3E**), which may be attributed to the H-bond between UOSC-1 and His244 and between UOSC-2 and His244 and Val248. Therefore, the lower RMSF values of the complexes indicate the lesser extent of conformational changes.

The compactness of inhibitor-enzyme complexes was measured by the Radius of gyration (Rg). Rg measures the distance of the region's parts from its centre of gravity. If a protein is stably folded, it will maintain a relatively steady value of Rg and if a protein unfolds, its Rg will change over the time. The Rg of the four inhibitor-protein complexes remained steady over the dynamics measurements (**Supplementary Figure 3H-L**). UOSC-2, 13 and 14 showed Rg ~2.055nm which is less than the protein alone, while UOSC-1 showed Rg similar to the protein alone. These results indicate the stabilization and non-significant conformational changes in the structures of all complexes. Hydrogen bonds play an important role in stabilizing a protein-ligand complex, where higher number of intermolecular

hydrogen-bonds results in a greater stability. In the present study, the analyses of hydrogen bond interactions were performed to test the stability of the aforementioned promising fungal tyrosinase inhibitors. Studying the H-bonds over 10 ns indicated that UOSC-1, 2, 13 and 14 showed stable and strong H-bonds with the tyrosinase enzyme much better than kojic acid (**Supplementary Figure 3H-L**). UOSC-2 illustrated the most stable and maintained H-bonds, indicating its superiority and promising anti-melanin activity of the fungus (**Supplementary Figure 3I**).

S3

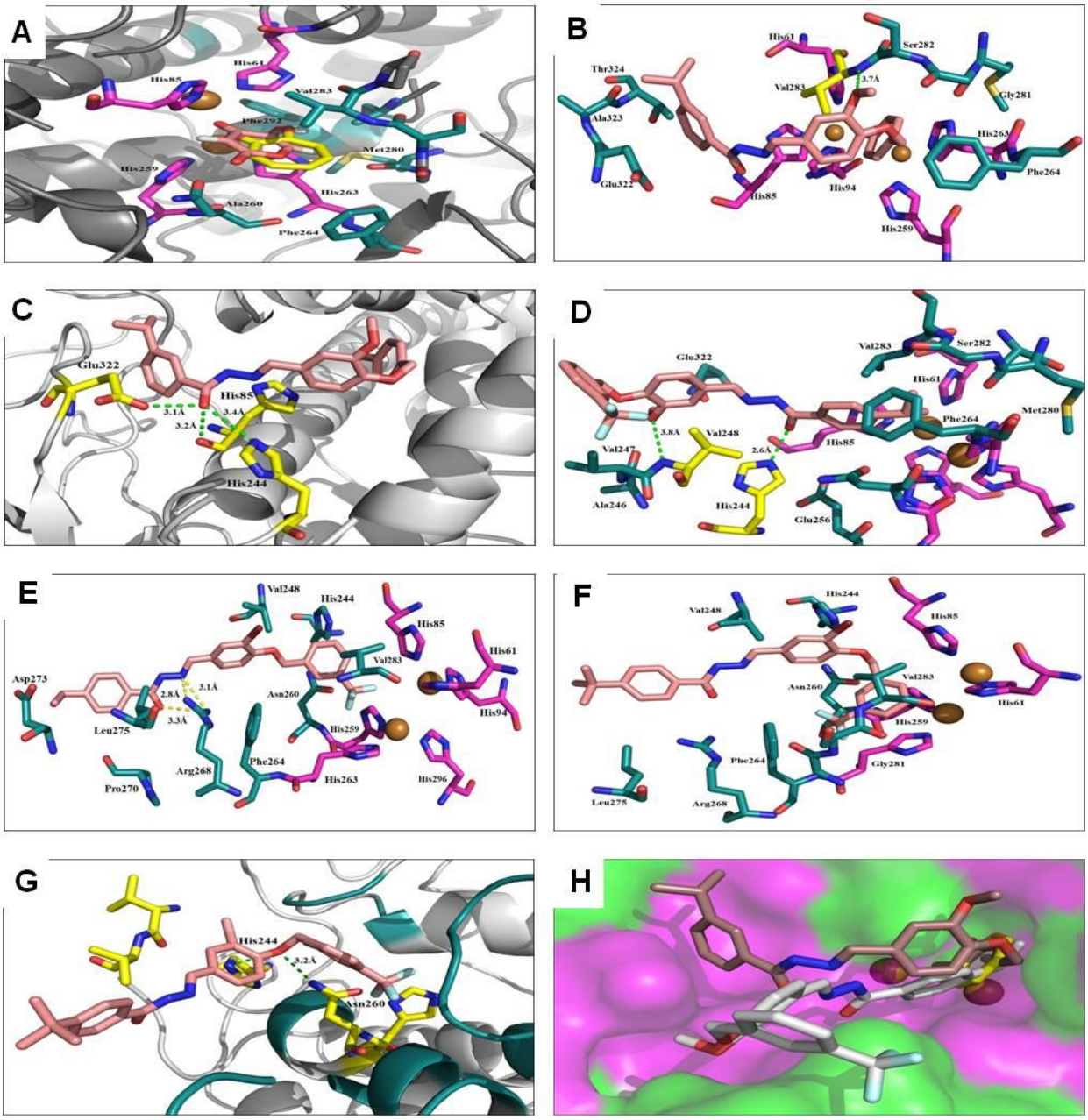

Supplementary Figure 1. Interaction of native ligands tropolone and kojic acid and UOSC-1, 2, 13 and 14 within the active site of mushroom tyrosinase. (A) Illustrated interaction of native ligand tropolone (yellow stick) and kojic acid (light pink stick) within the active site of mushroom tyrosinase (PDB:2Y9X). Copper ions represented as cuprous sphere surrounded with Histidine residues (pink stick). **(B)** Illustrated interactions of compound 1(light brown stick) with residues (dark green stick. NH- Val 283 (yellow stick) showed H-bond (green dot) with OCH_3 of

compound 1. **(C)** Illustrated snapshot of molecular dynamics of compound 1 (light brown stick) interactions with residues (yellow stick). O-atom of C=O of compound 1 formed 3 H-bonds with His85, Glu322 and His244. **(D)** Illustrated interactions of compound 2 (light brown stick) with residues (dark green stick). Compound 2 showed H-bonds (yellow stick) with His244 and Val248. **(E)** Illustrated interactions of compound 13 (light brown sticks), with pocket residues (green stick. H-bonds represented as yellow dots. **(F)** Illustrated hydrophobic interactions of compound 14 (light brown stick) with residues (dark green stick). **(G)** Illustrated snapshot of MD simulation of compound 14 (light brown stick) with residues (yellow stick), O atom of compound 14formed two H-bonds with Asn260 and His244. **(H)** Binding mode of native ligand (yellow stick), compound 1 (brown stick) and compound 2 (white stick). The two compounds occupied the active centre similar to native ligand. Both compounds are so near to copper ions. The remaining of the two molecules' structure extended in the binding pocket, the surface represented as hydrophilic (pink), hydrophobic (green), neutral (white).

S4

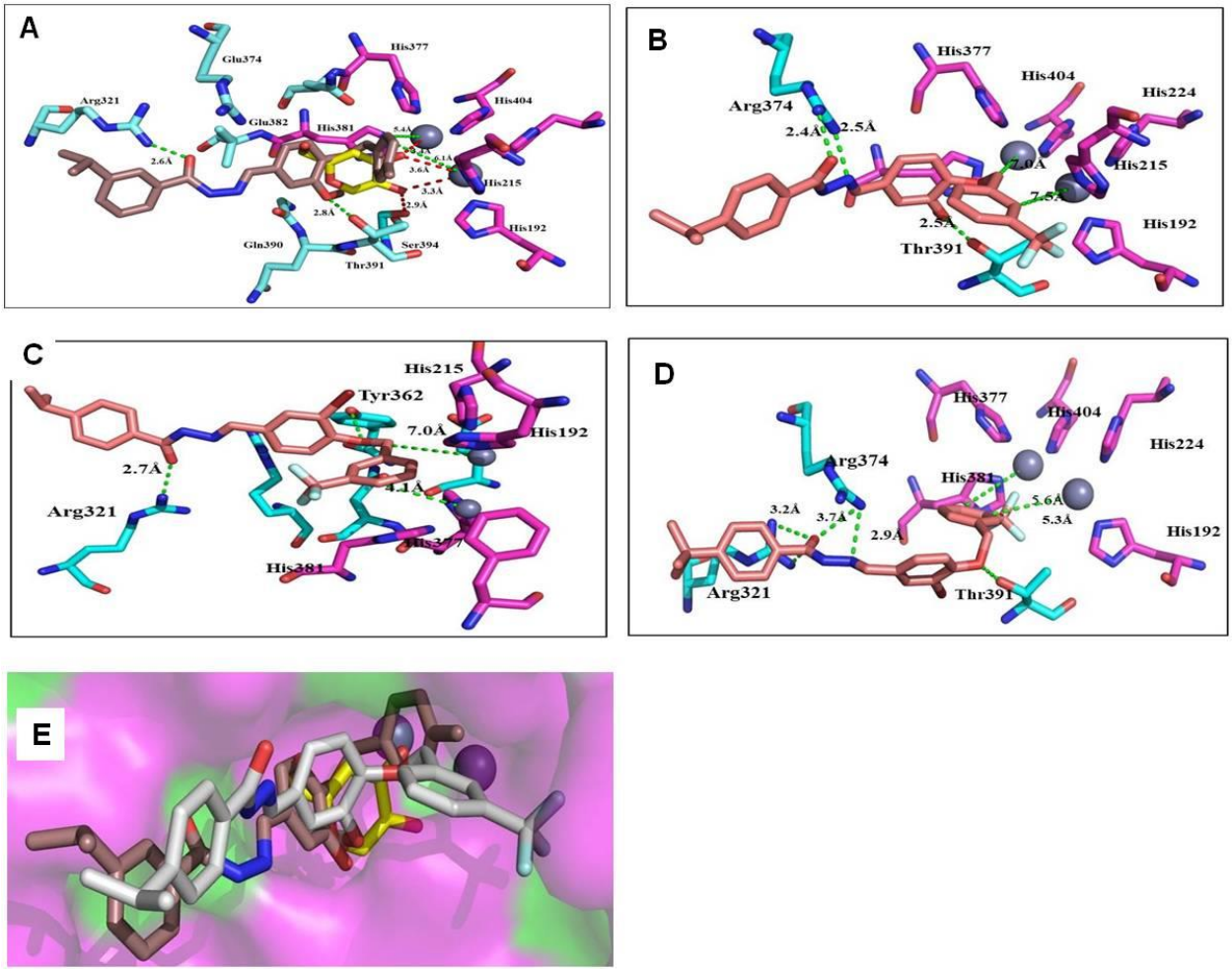

Supplementary Figure 2. Interactions of UOSC-1, 2, 13 and 14 and the native ligand kojic acid within the active site of human tyrosinase. (A) Illustrated interactions of UOSC-1 (light brown stick) within human tyrosinase active site (PDB:5M8M). **(B)** Illustrated interactions of UOSC-2. **(C)** Illustrated interactions of UOSC-13. **(D)** Illustrated interactions of UOSC-14. **(E)** Illustrated binding mode of UOSC-1(brown stick), UOSC-2 (white stick) and kojic acid (yellow stick). Human tyrosinase surface represented as hydrophilic (pink), hydrophobic (green) and neutral (white). Zinc ions represented as violet spheres, histadines ligands represented as pink stick and pocket residues are represented as cyan stick. Kojic acid, the native ligand represented as yellow stick. H-bonds between compound #1 and active site are green dots while H-bonds between kojic acid and pocket are red dots. H-bonds between kojic acids and Zn ions are shorter than the H-bonds between UOSC-1and Zn ions. The H-bonds between UOSC-2 and Zn ions are not in accepted H-bond length.

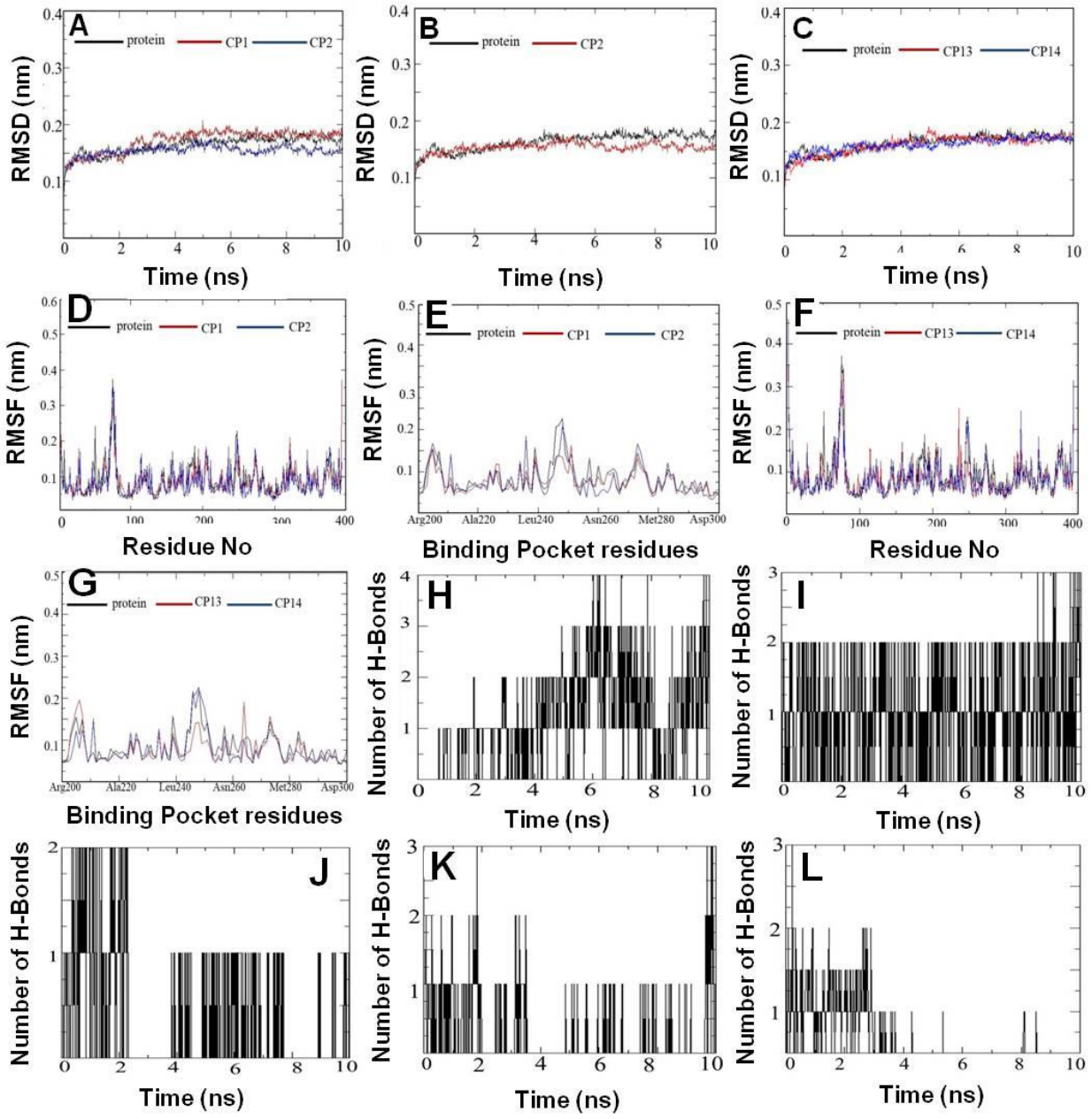

Supplementary Figure 3. Molecular Dynamics (MD) simulation of the newly-designed tyrosinase inhibitors. **(A-C)** Illustrated RMSD values over 10ns simulations of **(A)** the protein (black), UOSC-1 (red) and UOSC-2 (blue), **(B)** the protein (black) and UOSC-2 (red) and **(C)** the protein (black), UOSC-13 (red) and UOSC-14 (blue). **(D-G)** Illustrated RMSF values in nm over 10 ns simulations. **(D)** RMSF of the protein (black), UOSC-1 (red), UOSC-2 (blue). **(E)** RMSF of the binding pocket's residues of the protein (black) and compound #1 (red) and UOSC-2 (blue).

(F) RMSF of the whole protein (black), and UOSC-13 (red) and UOSC-14 (blue). **(G)** RMSF of the binding pocket's residues of the protein (black) and UOSC-13 (red) and UOSC-14 (blue). **(H-L)** H-bonds interaction over 10ns MD simulation of **(H)** UOSC-1, **(I)** UOSC-2, **(J)** UOSC-13, **(K)** UOSC-14 and **(L)** Kojic Acid.

S6

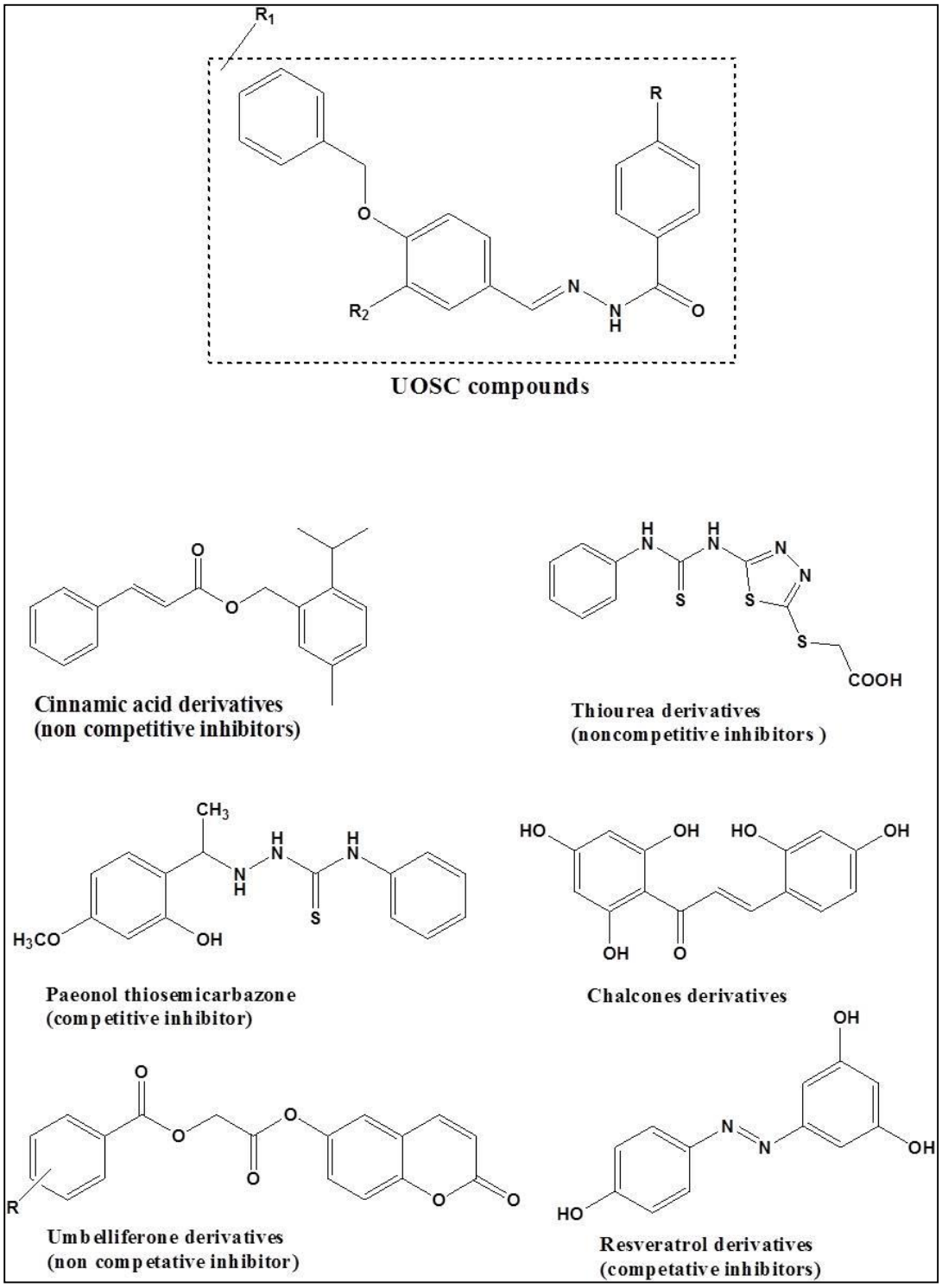

Supplementary Figure 4. Structural comparison between USC compounds and other reported synthetic and natural anti-melanin compounds.

S7

Spectral Data of compound UOSC2

^{13}CNMR

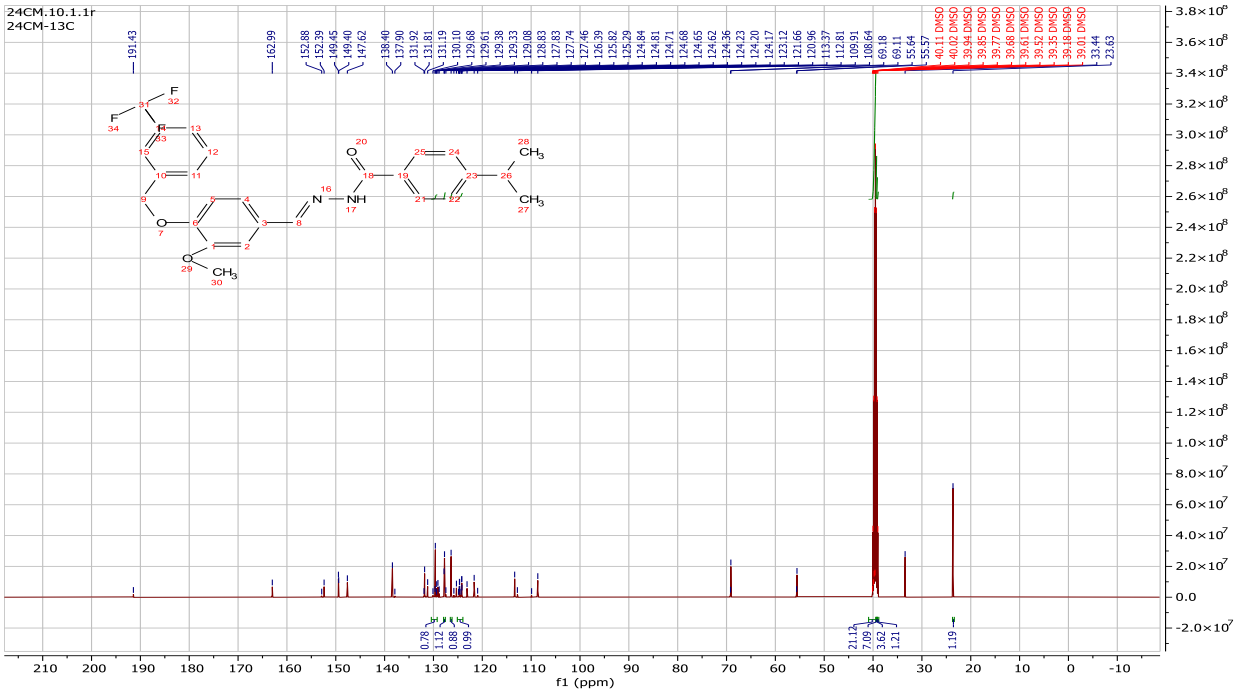

^{1}HNMR

HNMR

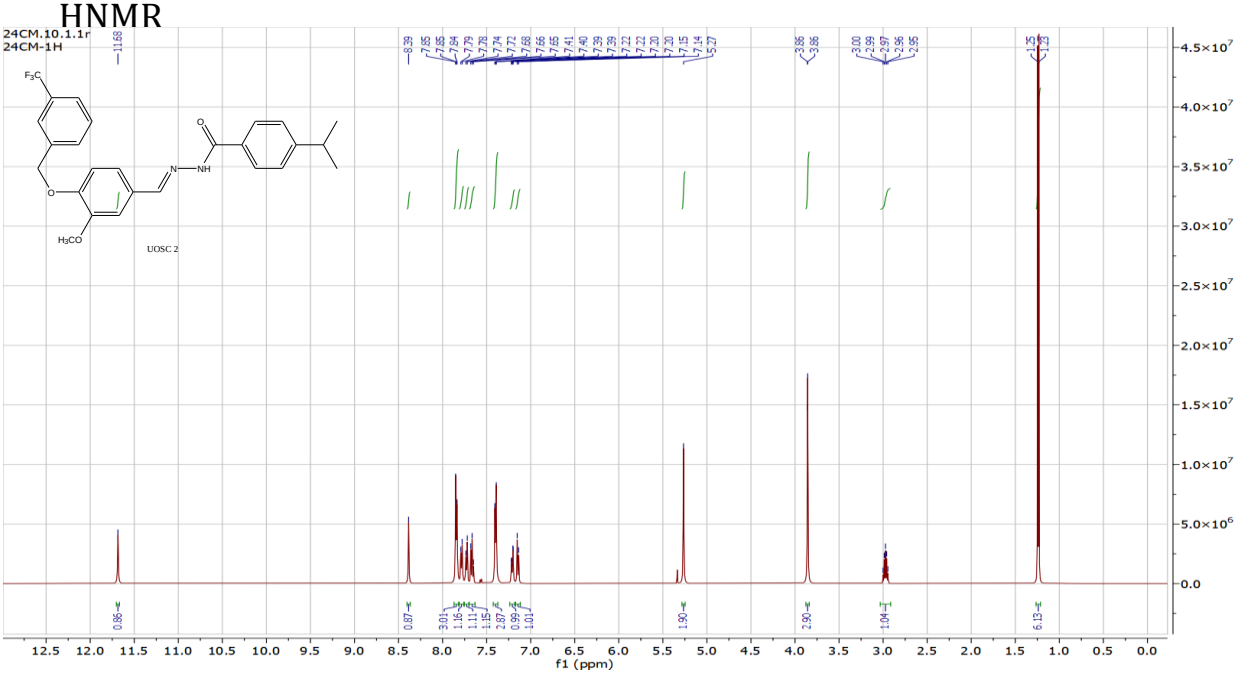

Mass

Mass

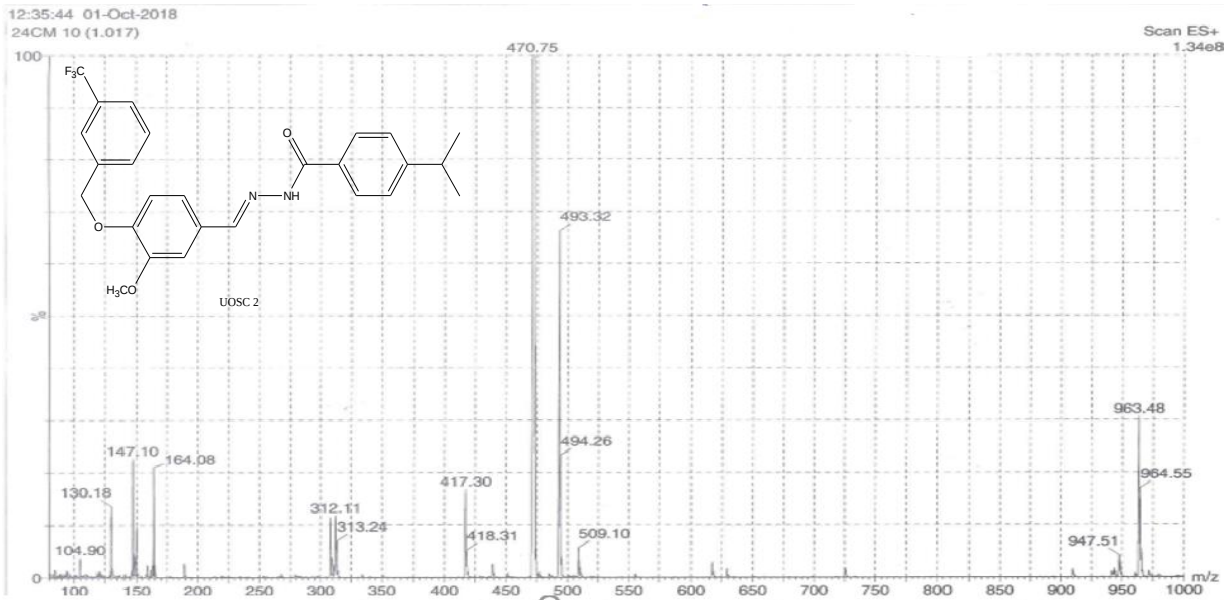
12:35:44 01-Oct-2018
24CM 10 (1.017)
Scan ES+
1.34e8
100
%
0
470.75
493.32
963.48
494.26
964.55
147.10
164.08
417.30
130.18
312.11
313.24
418.31
509.10
947.51
104.90
100
150
200
250
300
350
400
450
500
550
600
650
700
750
800
850
900
950
1000
m/z
F3C
O
N
NH
O
H3CO
UOSC 2